A Vertically Integrated Micromachined Filter

Lee Harle and Linda P. B. Katehi, *Fellow, IEEE*

***Abstract*—A 10-GHz filter constructed of slot-coupled micromachined cavities in silicon is presented. The novel character of the filter lies in its structure, which consists of a microstrip feed to cavities via slot apertures and three vertically stacked slot-coupled cavities. The cavities are essentially reduced-height waveguide resonators. The measured results are presented and compared to a finite-element-method model. The simulated model has a bandwidth of 4% with an insertion loss of 0.9 dB at 10.02 GHz. The measured filter yields a 3.7% bandwidth with a deembedded insertion loss of 2.0 dB at 10.01 GHz. Various loss mechanisms are examined to explain the difference between simulated and measured insertion loss.**

***Index Terms*—Filter, micromachined cavity, microwave.**

I. Introduction

MICROWAVE filters are traditionally made of metallic rectangular or cylindrical waveguides that yield a high quality-factor Q and excellent performance, but are heavy in weight and difficult to integrate with monolithic circuits. Planar filter configurations have been investigated over the past few years and have been found to have a performance limited only by conductor losses of the resonator sections, but are limited to relatively wide bandwidth [1], [2]. Transmission lines tend to be lossy in planar form and, hence, have a low Q [3]. The unloaded Q of a generalized transmission line is inversely proportional to guide wavelength. For a high Q, a small guide wavelength is needed, which requires higher dielectric constants. To avoid loss to substrate modes due to these higher dielectric constants, thinner substrates and narrower transmission lines must be used. However, the narrower the transmission line, the higher the ohmic loss. Excellent work has been done in the area of micromachined planar filters, where the micromachining has been employed to produce membrane-supported microstrip lines and micropackaging. These techniques yield reduced dielectric loss, reduced dispersion, reduced radiation loss, and better isolation between circuits [4]–[7]. In this paper, however, the micromachining technique is used to produce the three-dimensional cavity, which is the resonant component of the filter.

A study at the Jet Propulsion Laboratory (JPL), Pasadena, CA, has shown the ohmic loss of micromachined waveguides at 75–110 GHz to be 0.133 dB/cm, which is comparable to machined metallic waveguides [8]. Micromachined cavity resonators can be the building blocks for a filter design that is low loss, narrow in bandwidth, and small in size, and can be integrated into a monolithic circuit design.

A low-loss high-Q resonator cavity fabricated in a planar environment using standard micromachining techniques was demonstrated in [9]. This paper presents the first demonstration of a three-pole filter using this high-Q micromachined resonator. A filter synthesis is developed and the validity of the process is demonstrated as a filter that consists of three slot-coupled vertically integrated resonators, as shown in Figs. 1 and 2. The reduced-height micromachined waveguide is a unique three-dimensional concept in silicon. A high-Q filter constructed of these resonators yields high power-handling capabilities as the surface currents are distributed over a large conductor area.

II. Design and Simulation

The design is accomplished with the aid of Ansoft's High Frequency Structure Simulator (HFSS) FEM modeling package.[1] A Chebyshev filter with a 0.1-dB ripple, three resonators, and a 4% bandwidth is chosen as a demonstration vehicle for the proposed concept.

The external Q, i.e., Q_e, is defined as the Q that would result if the resonant circuit was loss free and if only loading by the external circuit was present [10]. This relationship can be used to determine external coupling. First, Q_e values are determined using

$$Q_{e1} = \frac{g_0 g_1 \omega_1'}{\Delta\omega} \quad Q_{en} = \frac{g_n g_{n+1} \omega_1'}{\Delta\omega} \tag{1}$$

where Q_{e1} is the external coupling from the input microstrip line to the circuit, Q_{en} is the external coupling from the nth or last resonator to the output microstrip line, ω_1' is the prototype corner frequency (taken to be $\pi/2$), $\Delta\omega$ is the fractional bandwidth, and the $g_j's$ are the parameters of the low-pass prototype [3]. For an odd number of resonators, as in this study, the g values are symmetric, thus, $Q_{e1} = Q_{en}$.

Through the simulations of a microstrip line coupled via a slot to the micromachined cavity [see HFSS model cross section in Fig. 3(a)], the relationship between the length of the external slots and the phase response of S_{11} is determined using

$$Q = \frac{f_0}{\Delta f} \tag{2}$$

where Q is equal to the unloaded Q, i.e., Q_u, for very weak coupling and the loaded Q, i.e., Q_l, for stronger coupling, Δf is the

Manuscript received May 9, 2001. This work was supported by the Jet Propulsion Laboratory under the Center for Integrated Space Microsystems/System-on-a-Chip Project.

L. Harle is with the Department of Electrical Engineering Computer Science, Radiation Laboratory, The University of Michigan at Ann Arbor, Ann Arbor, MI 48109-2122 USA (e-mail: leeharle@engin.umich.edu).

L. P. B. Katehi was with the Department of Electrical Engineering Computer Science, Radiation Laboratory, The University of Michigan at Ann Arbor, Ann Arbor, MI 48109-2122 USA. She is now with the Schools of Engineering, Purdue University, West Lafayette, IN 47907 USA.

Publisher Item Identifier 10.1109/TMTT.2002.802317.

[1]*HP85180A HFSS*, ver. 2.0.55, Ansoft Corporation, Pittsburgh, PA, 1999.

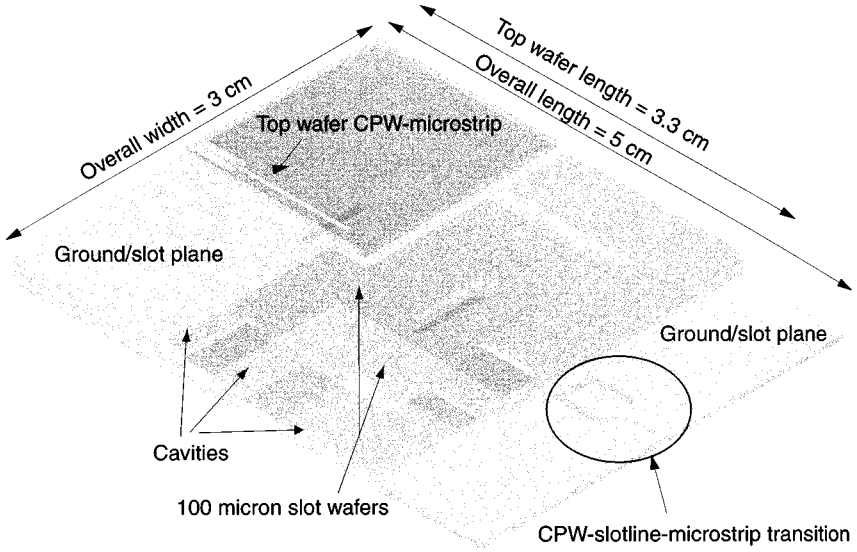

Fig. 1. Cutaway view of CPW-microstrip fed slot-coupled three-cavity filter. View is to scale.

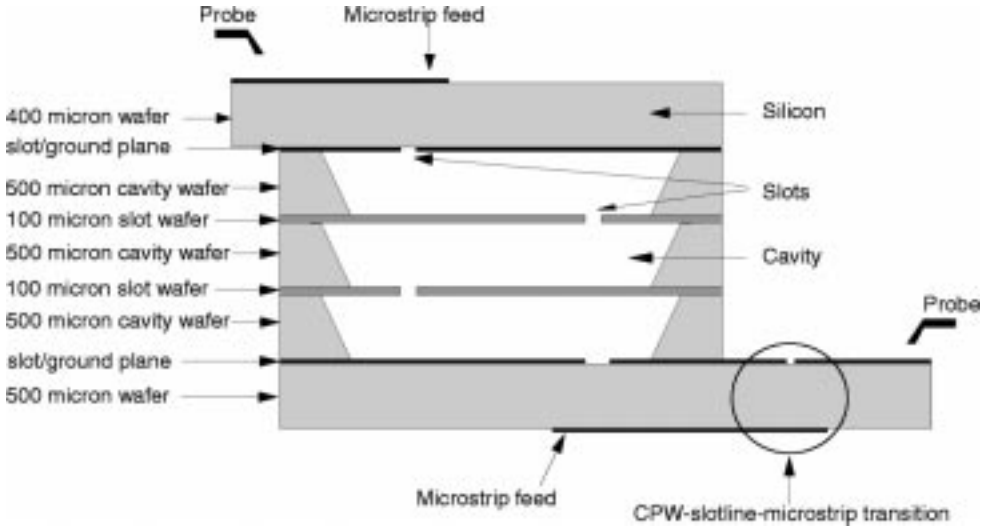

Fig. 2. Side view of three-cavity filter. View is not to scale.

difference in frequency between $+90^\circ$ and -90° phase of S_{11}, and f_o is the resonance of the coupled resonator at 0° phase. Q_l approaches Q_e as coupling increases, which occurs with an increase in slot length. Simulations are run for slots of constant width, but varying length,and the external quality factor Q, as determined by (2), is plotted versus slot length (Fig. 4). Nonlinear regression is used to determine a curve fitted to the data and a slot of 5.6 mm $\times$ 0.635 mm is chosen. Hence, external coupling, as determined by slot length, is related to Q_e from (2), which is related to the desired prototype Q_e, as determined by (1).

The desired internal coupling coefficients $k_{j,j+1}$ between the j^{th} and $j^{\text{th}}+1$ resonators are calculated using

$$k_{j,j+1} = \frac{\Delta\omega}{\omega_1'}\sqrt{\frac{1}{g_j g_{j+1}}}. \tag{3}$$

The design of the internal coupling coefficient k is well understood (see Zaki *et al.* [12] and Hong *et al.* [13]). The coupling coefficient is defined in terms of equivalent-circuit elements, which can be related to the mode splitting that occurs for even- and odd-mode excitation when electric (or short-circuit) and magnetic (or open-circuit) walls are alternately placed at the plane of symmetry between the resonators. This relationship is given by

$$k = \frac{f_{\text{even}}^2 - f_{\text{odd}}^2}{f_{\text{even}}^2 + f_{\text{odd}}^2} \tag{4}$$

where f_{even} denotes the lower resonance frequency and f_{odd} denotes the upper resonance frequency.

Through the simulation of two coupled cavities fed simply by waveguides via slots [see HFSS model cross section in Fig. 3(b)], the relationship between the length of the internal slot and the pole-splitting of the resonance frequency is determined. Simulations are run for slots of constant width, but varying length, and the coupling coefficient k, as determined by (4), is plotted versus slot length (Fig. 5). Nonlinear regression is used to determine a curve fitted to the data and a slot of

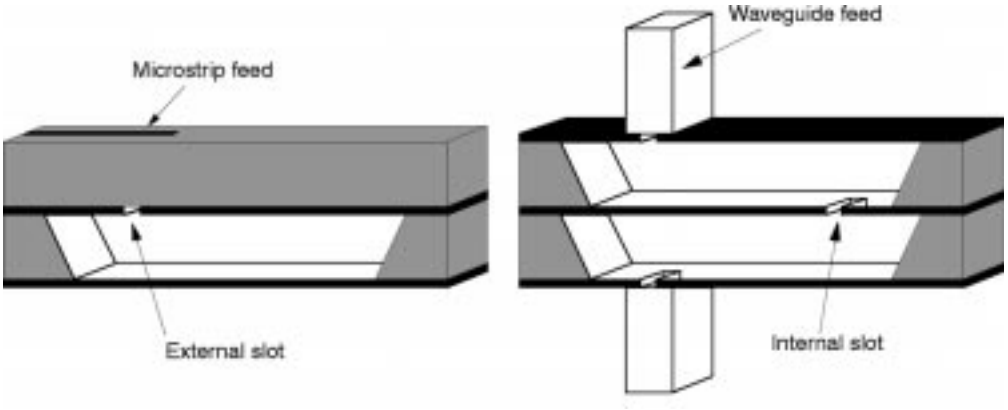

(a) (b)

Fig. 3. HFSS cross-sectional models for: (a) external quality factor Q_e and (b) internal coupling coefficient k.

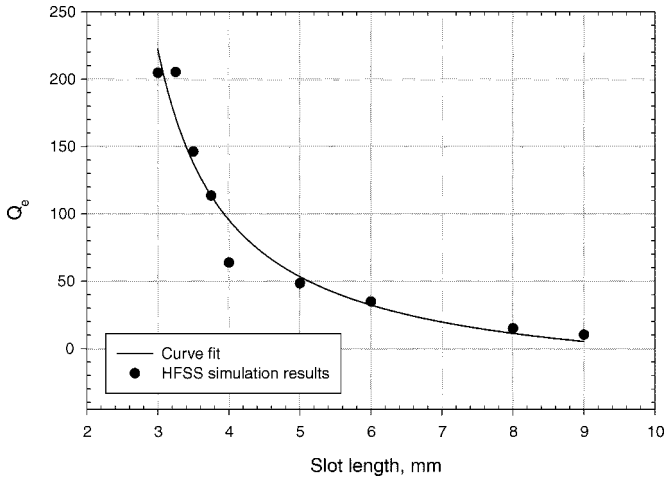

Fig. 4. External Q versus slot length, curve fit to HFSS simulation results. Slot width held constant at 0.635 mm.

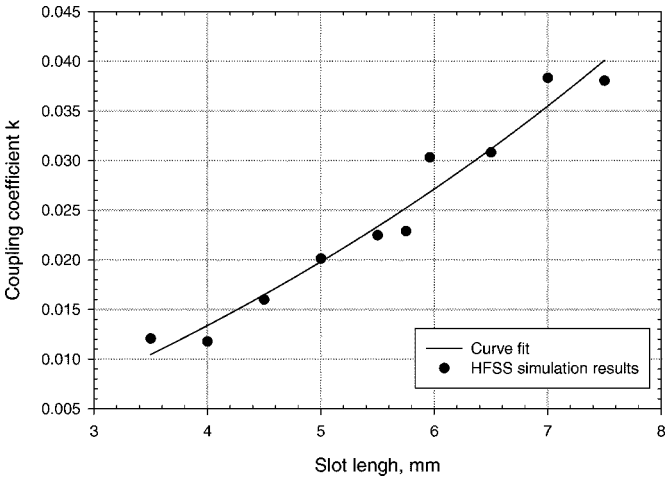

Fig. 5. Coupling coefficient k versus slot length, curve fit to HFSS simulation results. Slot width held constant at 0.706 mm.

5.921 mm $\times$ 0.706 mm is chosen. Hence, internal coupling, as determined by slot length, is related to k from (4), which is related to the desired prototype k, as determined by (3).

The 10-GHz resonant frequency of the dominant mode TE_{101} dictates the dimensions of the cavity by

$$f_{101} = \frac{c}{2\pi\sqrt{\mu_r \epsilon_r}} \sqrt{\left(\frac{m\pi}{a}\right)^2 + \left(\frac{n\pi}{b}\right)^2 + \left(\frac{l\pi}{d}\right)^2} \tag{5}$$

where a, b, and d are the width, height, and length of the cavity, respectively, and $m = l = 1$, $n = 0$ are the indexes for the 101 mode. A square cavity (2.12 $\times$ 2.12 cm^2) is chosen for maximum possible unloaded Q, as determined by

$$Q_{\mathrm{cond}} = \frac{(kad)^2 b\eta}{2\pi^2 R_s} \frac{1}{\left(2l^2a^3b + 2bd^3 + l^2a^3d + ad^3\right)} \tag{6}$$

where k is the wavenumber, η is the free-space impedance, R_s is the surface resistivity of the gold cavity walls, the index $l = 1$ for the dominant mode, a, b, and d are the cavity dimensions as stated above, and Q_{cond} is the Q of a cavity with lossy conducting walls. Q_u reduces to Q_{cond} for air-filled cavities [3].

With the slot lengths and cavity size determined, the complete filter is modeled in HFSS with the slots placed 1/4 of the cavity length from the sides and with a microstrip stub length of approximately $\lambda_g/6$ at 10 GHz for maximum coupling to the slot. The simulated results are shown in Fig. 6 with a bandwidth of 4% and insertion loss of 0.9 dB at 10.02 GHz. The theoretical insertion loss of a filter

$$\mathrm{IL} = 8.686 \frac{C_n}{\Delta\omega Q_u} \tag{7}$$

with $C_n = 1.6$, as determined by the number of resonator elements and passband ripple, and $Q_u = 565$, as determined by the size and conductivity of a single resonator cavity from (6), yields a theoretical best insertion loss of 0.6 dB [11]. The HFSS theoretical model is within the limit imposed by (7).

The HFSS modeled filter is identical to Fig. 1, but without a coplanar waveguide (CPW) to microstrip transition on either the top or bottom wafer. The model consists of seven silicon wafers. The top wafer is 400-μm thick and has a microstrip feed line on the top side coupled to a slot aperture in the ground plane on the bottom side. This slot feeds a cavity in a 500-μm wafer. A slot in a 100-μm wafer serves as the transition between the top and middle cavities and also between the middle and bottom cavities. The three cavities are identical. The bottom wafer is

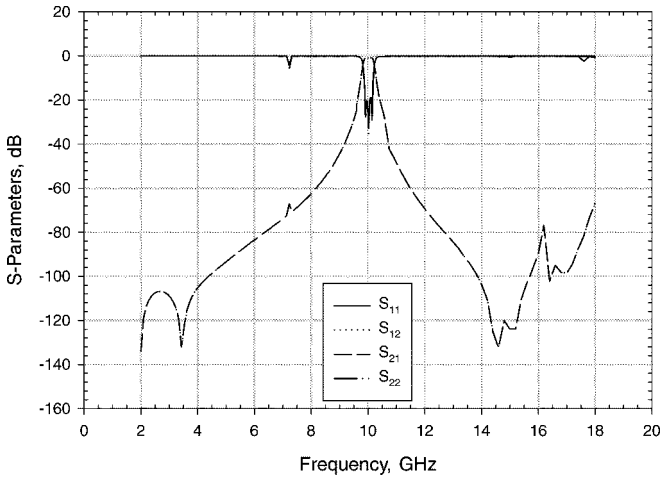

Fig. 6. HFSS simulation of three-cavity filter.

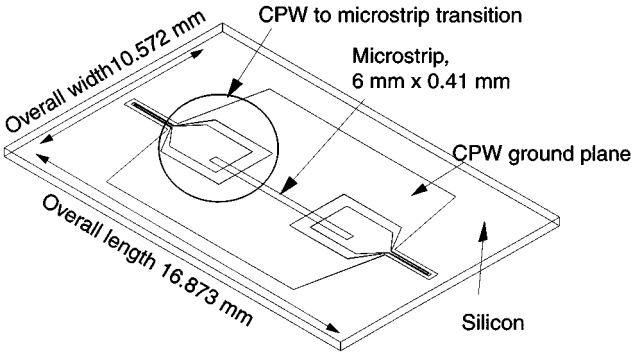

Fig. 7. CPW to microstrip transition in a back-to-back through-line configuration. The CPW is on the top of the wafer, the microstrip is on the bottom of the wafer.

500-μm thick with a microstrip on the bottom side and a slot aperture in the ground plane on the top side, coupling to the bottom cavity.

The model has microstrip feed lines on the top surface of the top wafer and on the bottom surface of the bottom wafer. However, the laboratory measuring facility requires that the feed lines for both ports be CPW and on the same side of the circuit. For this reason, it is necessary to design a transition for the bottom microstrip line to a CPW line on the top of the wafer after the fashion of [14] and as shown in Fig. 7. Several back-to-back through-line transitions (CPW to microstrip to CPW) are simulated in IE3D[2] and fabricated on high-resistivity 400-μm silicon wafers in order to determine the loss per transition and per length of microstrip line. The simulated and measured results for the filter frequency range of interest are shown in Fig. 8. The loss per transition is found to be 1.2 dB at 10 GHz. One of these transitions is used on the bottom wafer to transition the feed line as seen incorporated into the final filter design in Fig. 1.

The difference between measured and simulated results for the back-to-back through line is partially explained by the way in which IE3D models ohmic loss. To confirm that, a 50-Ω through line was modeled in IE3D and found to have a predicted loss of 0.16 dB/cm at 90 GHz. However, the same through line was fabricated, measured, and found to have 0.28-dB/cm loss at

[2]*Zeland IE3D*, ver. 5.01, Zeland Software, Fremont, CA, 1998.

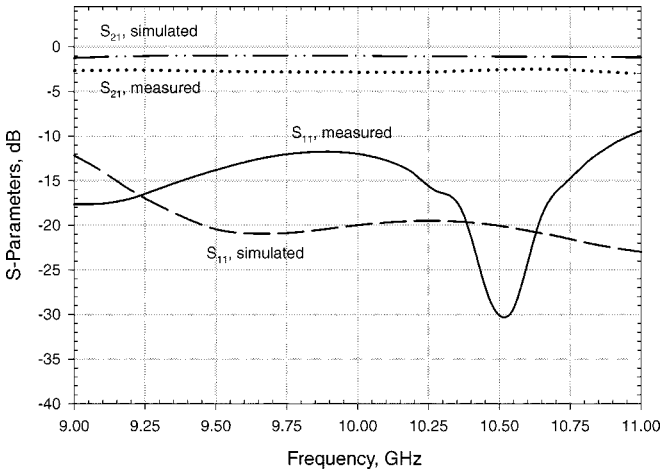

Fig. 8. Simulated and measured results for CPW to microstrip transition in a back-to-back through-line configuration.

90 GHz [15]. Although a finite conductivity of 4.1×10^7 S/m is used in the model presented in this paper, the program approximates the conductors by the surface impedance of an infinite conductor in the direction perpendicular to the flow of transverse current component and does not attempt to compute the fields inside the conductors [16].

III. Fabrication

The filter is fabricated using high-resistivity silicon wafers with $\epsilon_r = 11.7$. Thermally deposited SiO_2 is used as an etch mask. The micromachined cavities are etched using tetramethyl ammonium hydroxide (TMAH) wet chemical anisotropic etching. The internal coupling slots are etched using potassium hydroxide (KOH) wet chemical anisotropic etching due to its ability to define small fine features. The microstrip lines, CPW lines, and top and bottom wafer ground/slot planes are gold electroplated to approximately 3 μm (3–4 skin depths at 10 GHz). All surfaces of the etched slot and cavity wafers are gold electroplated to a similar depth. The wafers are aligned and thermal-compression bonded in the vacuum bond chamber of an EV 501 Manual Wafer Bonder at 350 °C with 750 N of pressure in a vacuum chamber [17], [18]. The overall dimensions of the finished circuit are approximately 5 cm long $\times$ 3 cm wide $\times$2600 μm high, as illustrated in Fig. 1.

IV. Results and Discussion

The finished filter is measured on an HP8510C Network Analyzer[3] using a thru-reflect-line (TRL) calibration [19]. The CPW calibration moves the reference planes to the CPW taper transition on both the top and bottom wafers. The overall shape of the filter response compared favorably with the simulated model. The measured losses were found to be higher than expected. These losses are due in part to the CPW–microstrip transition and line lengths. As mentioned above, the transition and line losses are determined from through lines of various lengths. Also, equipment malfunction during the bonding caused an unexpected rapid rise in temperature, which created a gold-silicon

[3]Agilent Technol., Palo Alto, CA.

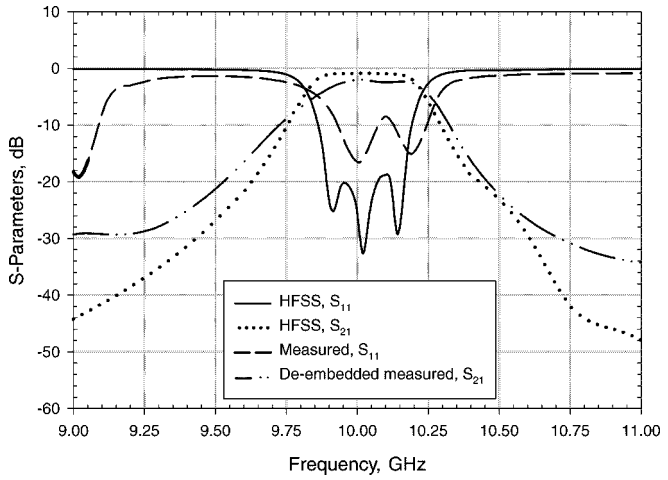

Fig. 9. Expanded plot from 9–11 GHz comparing simulated and deembedded measured return and insertion losses.

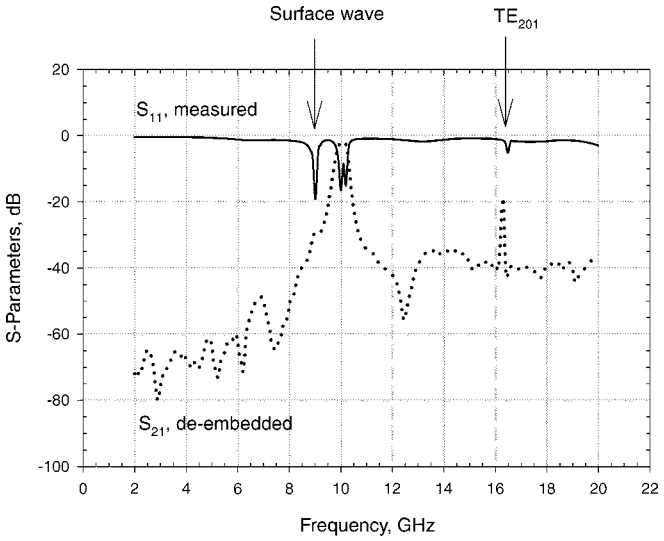

Fig. 10. Deembedded measurement of three-cavity filter. Note the resonances at 9 and 16.5 GHz.

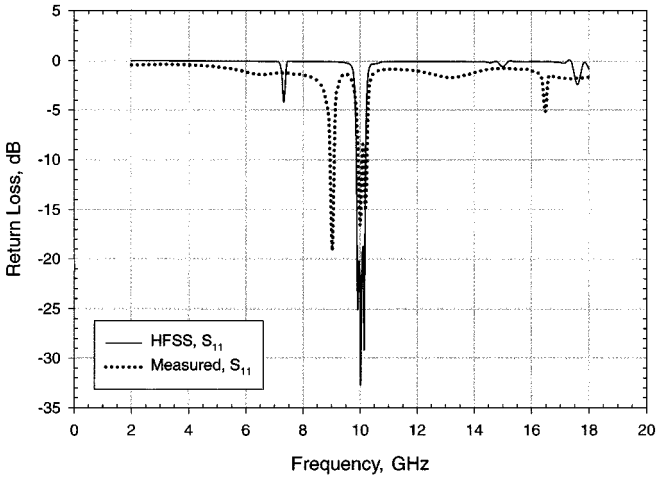

Fig. 11. Simulated and measured return loss.

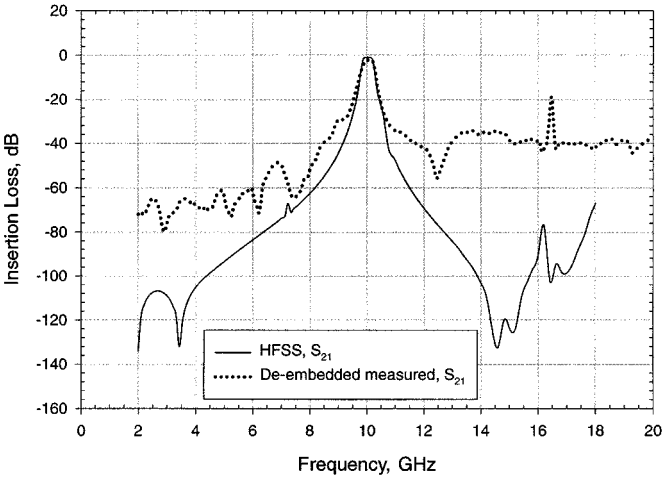

Fig. 12. Simulated and deembedded insertion loss.

eutectic and resulted in additional loss. A detailed investigation into the transmission line performance of a gold-silicon eutectic indicated that a reduction in the conductivity of the gold was induced by the creation of the eutectic. In the future, a lower target bond temperature will be used.

All of these losses were calculated as a function of frequency and deembedded from the measured insertion loss data. An expanded plot of a comparison of the simulated and deembedded measured insertion-loss results is shown in Fig. 9 with a bandwidth of 3.7% and a calibrated deembedded insertion loss of 2.0 dB at 10.01 GHz, with reference planes located approximately at the center of the external slots. The measurement repeatability error is on the order of ± 0.1 dB. Despite the deembedding of the feed-line loss, the insertion loss of the filter is more than 1 dB higher than the simulated model insertion loss of 0.9 dB. Each of the three cavities has a gold-plated surface area of approximately 9 cm^2. The reduction in conductivity induced by the gold-silicon eutectic on these surfaces likely accounts for this discrepancy.

The losses due to the CPW–microstrip transition and the gold-silicon eutectic were not deembedded from the measured return-loss data. The difference between simulated results and measured data are attributed to these losses.

Fig. 10 shows the deembedded measurement of the filter from 2 to 20 GHz. Out-of-band insertion loss is around 60 dB below and 40 dB above the passband, while the rejection above the passband was expected to be at least 20 dB lower. The difference between measured and expected values is attributed in part to excitation of spurious surface waves in the substrates, as described below, and is in part due to noise in the measurement equipment.

As shown in Fig. 10, several resonances are observed in the measured data. To understand these resonances, the transcendental equations for a grounded dielectric slab, representing the top microstrip wafer, are solved [3]. It is found that, at 9 GHz, a TM_0 surface wave with a zero cutoff frequency has a resonance in the top microstrip wafer, which behaves like a dielectric cavity. The surface wave can be launched from the radiating stub end of the microstrip (refer to Fig. 1). Simply changing the wafer dimensions and adding packaging can eliminate or move this resonance to another frequency. The resonance at 16.5 GHz is attributed to the TE_{201}, the next higher order cavity mode.

For ease of comparison, the simulated and measured return losses are shown in Fig. 11 and the simulated and deembedded insertion losses are shown in Fig. 12.

While the Q of this filter is not measured, the theoretical Q_u for the TE_{101} mode for a filter with air-filled cavities of this size is 565 from (6). A single weakly coupled cavity model in HFSS yields a Q_u of 558 at 10.175 GHz. Earlier work with rectangular cavities has yielded a measured Q_u of 506, compared to a theoretical Q_u of 526 [9], [20]. In addition to this work, it has been shown recently in [21] that a micromachined metallized cavity etched in 1000-μm silicon and weakly coupled yielded a measured Q_u of 890 at 20 GHz, compared to a theoretical value of approximately 1000. All of these results have demonstrated the ability to experimentally achieve Q_u very close to the theoretically calculated Q_u, using the appropriate conductivity value.

V. Conclusion

A multiple-pole micromachined vertically integrated bandpass filter has been successfully demonstrated for the first time. It is lightweight, of compact size, and may be easily integrated into a monolithic circuit. Loss is introduced because measurement of the circuit requires complex feed structures and the gold surfaces suffered a loss of conductivity during fabrication. In spite of these issues, the measured results show a filter response that is otherwise in very good agreement with the simulated model.

References

[1] T. M. Weller, L. P. B. Katehi, and G. M. Rebeiz, "A 250-GHz microshield bandpass filter," *IEEE Microwave Guided Wave Lett.*, vol. 5, pp. 153–155, May 1995.

[2] S. V. Robertson, L. P. B. Katehi, and G. M. Rebeiz, "Micromachined self-packaged W-band bandpass filters," in *IEEE MTT-S Int. Microwave Symp. Dig.*, Orlando, FL, May 1995, pp. 1543–1546.

[3] D. M. Pozar, *Microwave Engineering*. Reading, MA: Addison-Wesley, 1993.

[4] P. Blondy, A. R. Brown, D. Cros, and G. M. Rebeiz, "Low-loss micromachined filters for millimeter-wave communication systems," *IEEE Trans. Microwave Theory Tech.*, vol. 46, pp. 2283–2288, Dec. 1998.

[5] A. R. Brown and G. M. Rebeiz, "Micromachined micropackaged filter banks," *IEEE Microwave Guided Wave Lett.*, vol. 8, pp. 158–160, Apr. 1998.

[6] K. Takahashi *et al.*, "K-band receiver front-end IC integrating micromachined filter and flip-chip assembled active devices," in *IEEE MTT-S Int. Microwave Symp. Dig.*, Anaheim, CA, June 1999, pp. 229–232.

[7] C.-Y. Chi and G. M. Rebeiz, "A low-loss 20 GHz micromachined bandpass filter," in *IEEE MTT-S Int. Microwave Symp. Dig.*, Orlando, FL, May 1995, pp. 1531–1534.

[8] M. Yap, Y.-C. Tai, W. R. McGrath, and C. Walker, "Silicon micromachined waveguides for millimeter-wave and submillimeterwave frequencies," in *Proc. 3rd Int. Space Terahertz Technol. Symp.*, Ann Arbor, MI, Mar. 1992, pp. 316–323.

[9] J. Papapolymerou, J.-C. Cheng, J. East, and L. P. B. Katehi, "A micromachined high-Q X-band resonator," *IEEE Microwave Guided Wave Lett.*, vol. 7, pp. 168–170, June 1997.

[10] R. E. Collin, *Foundations for Microwave Engineering*. New York: McGraw-Hill, 1992.

[11] G. Matthaei, L. Young, and E. M. T. Jones, *Microwave Filters, Impedance-Matching Networks and Coupling Structures*. New York: McGraw-Hill, 1964.

[12] K. A. Zaki and C. Chen, "Coupling of nonaxially symmetric hybrid modes in dielectric resonators," *IEEE Trans. Microwave Theory Tech.*, vol. MTT-35, pp. 1136–1142, Dec. 1987.

[13] J. S. Hong and M. J. Lancaster, "Couplings of microstrip square open-loop resonators for cross-coupled planar microwave filters," *IEEE Trans. Microwave Theory Tech.*, vol. 44, pp. 2099–2109, Dec. 1996.

[14] T. Ellis, J.-P. Raskin, L. P. B. Katehi, and G. M. Rebeiz, "A wideband CPW-to-microstrip transition for millimeter-wave packaging," in *IEEE MTT-S Int. Microwave Symp. Dig.*, vol. 2, Anaheim, CA, June 1999, pp. 629–632.

[15] K. J. Herrick, "W-band three-dimensional integrated circuits utilizing silicon micromaching," Ph.D. dissertation, Dept. Elect. Eng. Comput. Sci., Univ. Michigan at Ann Arbor, Ann Arbor, MI, 2001.

[16] T. E. van Deventer, "Characterization of two-dimensional high frequency microstrip and dielectric interconnects," Ph.D. dissertation, Dept. Elect. Eng. Comput. Sci., Univ. Michigan at Ann Arbor, Ann Arbor, MI, 1992.

[17] "EV501 wafer bonding system," Electron. Visions Group, Shaerding, Austria, [Online]. Available: www.ev-global.com.

[18] K. J. Herrick and L. P. B. Katehi, "RF W-band wafer-to-wafer transition," *IEEE Trans. Microwave Theory Tech.*, vol. 49, pp. 600–608, Apr. 2001.

[19] R. B. Marks and D. F. Williams, *Multicat V1.00*. Boulder, CO: NIST, 1995.

[20] L. Harle, J. Papapolymerou, J. East, and L. P. B. Katehi, "The effects of slot positioning on the bandwidth of a micromachined resonator," in *Proc. 28th Eur. Microwave Conf.*, vol. 2, Oct. 1998, pp. 664–666.

[21] M. Hill, J. Papapolymerou, and R. Ziolkowski, "High-Q micromachined resonant cavities in a K-band diplexer configuration," *Proc. Inst. Elect. Eng.*, pt. H, vol. 148, pp. 307–312, Oct. 2001.

Lee Harle received the B.S. degree in physics from Indiana University, Bloomington, in 1996, the M.S.E. degree in electrical engineering from The University of Michigan at Ann Arbor, in 1998, and is currently working toward the Ph.D. in electrical engineering at The University of Michigan at Ann Arbor.

Her research is focused on micromachined cavity resonators in silicon and their applications to high-frequency filters and diplexers.

Linda P. B. Katehi (S'81–M'84–SM'89–F'95) received the B.S.E.E. degree from the National Technical University of Athens, Athens, Greece, in 1977, and the M.S.E.E. and Ph.D. degrees from the University of California at Los Angeles, in 1981 and 1984, respectively.

In September 1984, she joined the faculty of the Electrical Engineering and Computer Science Department, The University of Michigan at Ann Arbor, as an Assistant Professor, and then became an Associate Professor in 1989 and Professor in 1994. She has served in many administrative positions, including Director of Graduate Programs, College of Engineering (1995–1996), Elected Member of the College Executive Committee (1996–1998), Associate Dean For Graduate Education (1998–1999), and Associate Dean for Academic Affairs (since September 1999). She is currently the Dean of the Schools of Engineering, Purdue University, West Lafayette, IN. She has authored or co-authored 410 papers published in refereed journals and symposia proceedings and she holds four U.S. patents. She has also generated 20 Ph.D. students.

Dr. Katehi is a member of the IEEE Antennas and Propagation Society (IEEE AP-S), the IEEE Microwave Theory and Techniques Society (IEEE MTT-S), Sigma Xi, Hybrid Microelectronics, and URSI Commission D. She was a member of the IEEE AP-S AdCom (1992–1995). She was an associate editor for the IEEE Transactions on Microwave Theory and Techniques and the IEEE Transactions on Antennas and Propagation. She was the recipient of the 1984 IEEE AP-S W. P. King (Best Paper Award for a Young Engineer), the 1985 IEEE AP-S S. A. Schelkunoff Award (Best Paper Award), the 1987 National Science Foundation Presidential Young Investigator Award, the 1987 URSI Booker Award, the 1994 Humboldt Research Award, the 1994 University of Michigan Faculty Recognition Award, the 1996 IEEE MTT-S Microwave Prize, the 1997 International Microelectronics and Packaging Society (IMAPS) Best Paper Award, and the 2000 IEEE Third Millennium Medal.